Chemical Science

Accepted Manuscript

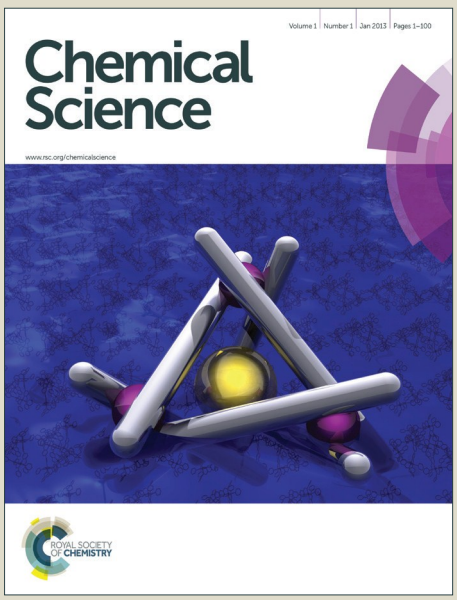

ROYAL SOCIETY OF CHEMISTRY

www.rsc.org/chemicalscience

Chemical Science

EDGE ARTICLE

Engineering electronic structure of Two-Dimensional Subnanopore nanosheet by Molecular Titanium-oxide Incorporation for Enhanced photocatalytic activity

Received 00th January 20xx,

Accepted 00th January 20xx

DOI: 10.1039/x0xx00000x

www.rsc.org/

Xiuli Lu[†a], Kun Xu[†a], Shi Tao[b], Zewei Shao[a], Xu Peng[a], Wentuan Bi[a], Pengzuo Chen[a], Hui Ding[a], Wangsheng Chu[b]*, Changzheng Wu[a]*, and Yi Xie[a]

Engineering electronic structure of two-dimensional (2D) nanomaterials entails unique physical and chemical properties. Although developed modification strategies have significantly expanded the applications of 2D nanomaterials, exploring new strategies to regulate the electronic structure of 2D nanomaterials is also expected. Herein, we highlight a new strategy to engineer the electronic structure of 2D subnanoporous nanomaterials. As a proof of concept, based on controllable subnanopore engineering by molecular titanium-oxide incorporation, electronic band structure of 2D graphitic carbon nitride nanosheets (CN) has been efficiently tuned with enhancement of visible light absorption as well as separation and migration rate of photo-excited charge carriers, exhibiting significantly improved photocatalytic activity under visible light irradiation. Our work opens a new door to engineering the intrinsic properties of 2D subnanoporous nanomaterials.

Introduction

Two dimensional (2D) nanomaterials are of great interest due to their 2D confined structure which brought exotic physical properties.[1-6] Recently, enormous efforts have been made to regulate the electronic structure of 2D nanomaterials in order to endow them with new functionalities or further enhance their intrinsic physical and chemical properties.[7-19] Generally, surface modification, defect engineering, and heteroatom doping are well known approaches to engineer intrinsic electronic structure of 2D nanomaterials.[8,9] For example, modification of various ions (i.e. F^-, H^+, Cl^- and so on) on the surface of 2D nanomaterials can effectively modulated their carries concentrations, bringing about new physicochemical properties.[10-15] Other modulation strategies such as defect engineering and heteroatom doping, have been widely applied to achieve synergic advantages of optimized electrical properties and higher chemical activity, holding promise for the enhancement of their catalytic performance.[16-20] Although substantial progresses have been made, developing new strategies for tuning electronic structure of 2D nanosheets is also expected.

2D polymers with subnanoporous structure have shown promising application in various fields such as bioimaging, nanoelectonic and catalysis attributing to their highly thermal stable and easier adjustment electronic structure.[21-26] Comparing with traditional inorganic 2D materials, the 2D microporous polymer (2D-MP) own the unique periodic vacancies (also called as "subnanopores") in their lattice.[23] These unique nanometer-sized pores in the 2D-MP could provide a new opportunity for modifying the electronic structure of 2D nanomaterials as well as remaining the integrity of their matrix. Herein, taking 2D graphitic carbon nitride (CN) as a material model, we develop a controllable subnanopore engineering strategy to regulate the electronic structure of 2D-MP nanosheets while not influence the pristine matrix structure of polymer. In our case, the subnanopore was incorporated by molecular titanium-oxide group, which was highly homogenously dispersed in the 2D CN framework. And titanium-oxide incorporation in subnanopores of CN has efficiently tuned the electronic band structure of 2D CN, bringing effective improvement of visible light absorption and the separation as well as migration rate of photo-excited charge carriers. As a result, 2D CN with molecular titanium-oxide incorporation shows enhanced photocatalytic activity under visible light irradiation compared with pure 2D g-CN. Our work provides a new way to engineering the intrinsic physical properties of 2D nanomaterials.

As demonstrated in **Figure 1A**, the controllable subnanopore engineering in 2D CN by molecular titanium-oxide incorporation (TiO-CN) was achieved by a simple "bottom-up" polycondensation of precursors which contain dicyandiamide (DICY) and titanium oxide ion. In detail, $TiCl_4$ and DICY were firstly dissolved in cooled ammonium chloride solution, forming a colorless and transparent aqueous solution. During the dissolving process, $TiCl_4$ was rapidly hydrolyzed to TiO^{2+}. It needs noted that the cooled ammonium chloride solution could prevent the $TiOCl_2$ molecular further hydrolyzing into H_2TiO_3 nanoparticle. Then, the whole solution was

[a] *Hefei National Laboratory for Physical Sciences at the Microscale, iChEM (Collaborative Innovation Center of Chemistry for Energy Materials), Hefei Science Center (CAS), and CAS Key Laboratory of Mechanical Behavior and Design of Materials , University of Science & Technology of China Hefei, Anhui 230026 (P. R. China)*
E-mail: czwu@ustc.edu.cn
[b] *National Synchrotron Radiation Laboratory University of Science & Technology of China Hefei, Anhui 230029 (P. R. China)*
E-mail: chuws@ustc.edu.cn
† These authors contributed equally to this work
† Electronic Supplementary Information (ESI) available: Experimental and characterization. See DOI: 10.1039/b000000x/

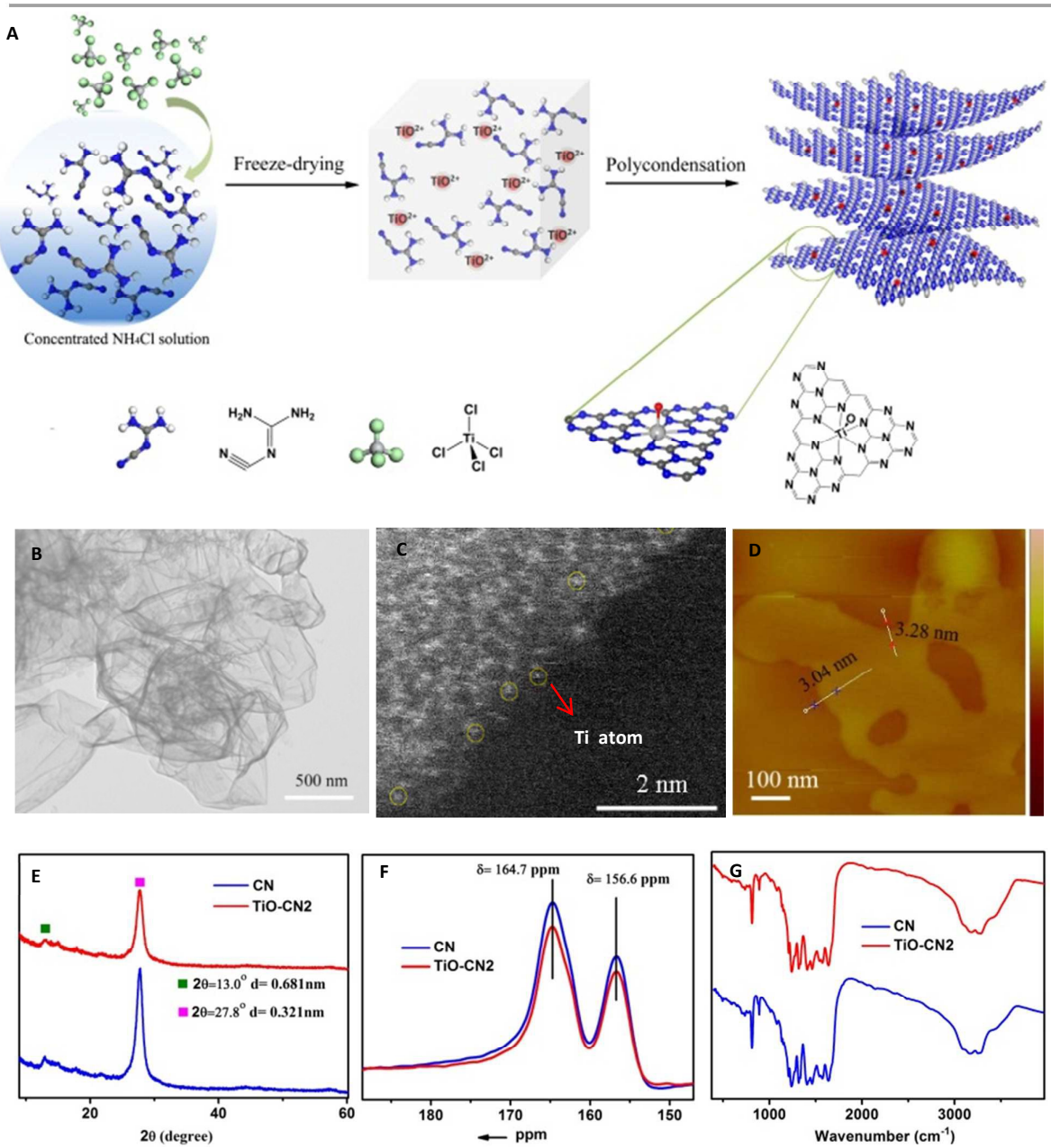

Fig. 1 (A) The Schematic illustration for the synthesis of TiO-CN from "bottom-up" polycondensation of the designed precursors. (B) TEM, (C) HAADF-STEM, (D) AFM image of TiO-CN2 nanosheet. (E) XRD patterns of CN and TiO-CN2 nanosheets. (F) The solid state ^{13}C NMR spectra of 2D CN and TiO-CN2 (G)IR spectra of CN and TiO-CN2.

freeze-dried to promise the fully mixture of DICY with TiO^{2+}, and finally the white solid powder was obtained. After that, the white powder was annealed at 550 ^{o}C for 4 h in a quartz container to get the final TiO-CN samples. Interestingly, CN nanosheets with gradual concentration of titanium-oxide incorporation could be easily controlled by tuning the amount of $TiCl_4$. According to the amount of molecular titanium-oxide incorporation in the subnanopores, the TiO-CN samples can be denoted as TiO-CN1, TiO-CN2 and TiO-CN3. The pure 2D g-CN was obtained without adding $TiCl_4$, denoted as CN.

Results and discussion

To unravel the microscopic morphologies of TiO-CN nanosheet, scanning electron microscopy (SEM), transmission electron microscopy (TEM), and atomic force microscopy (AFM) were carried out. SEM images of TiO-CN show uniform 2D nanosheets with obvious corrugations and porosities (Figure S3). The corresponding TEM image in Figure 1B also verifies the clean ultrathin nanosheet with a sheet-like morphology as that of CN. The AFM image revealed that the thickness of TiO-CN2 nanosheet (one of the TiO-

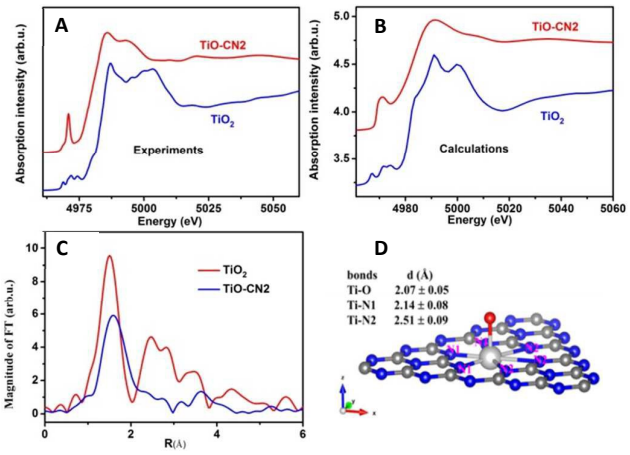

Fig. 2 (A, B) Experimental and calculated Ti k-edge XANES spectra of the prepared TiO-CN2 compared with the anatase TiO_2 powder. (C) FT-EXAFS comparison between the prepared sample and the standard anatase TiO_2. (D) The illustration of the detailed TiO-CN structure.

CN samples) is about 3~3.3 nm. Furthermore, EDX mapping analyses were performed to identify the distribution of molecular titanium-oxide in the matrix of 2D CN. As exhibited in Figure S7, the elemental mapping images reveal that the homogeneous distribution of carbon, nitrogen, titanium and oxygen in the whole ultrathin nanosheet. The results indicated that the titanium-oxide was highly homogenously dispersed in the framework of CN. The HAADF-STEM image of the TiO-CN2 nanosheet also confirmed that the titanium-oxide was homogenously dispersed in the framework of CN as shown in Figure 1C and Figure S5. And at the edge of the TiO-CN nanosheets where the yellow circles noted, we could clearly identify that the element Ti existed as isolated atom with atomic size, suggesting that isolated titanium-oxide species was coordinated in the subnanopores of CN. All above characterization results clearly demonstrated that 2D TiO-CN was successfully obtained by subnanopore engineering with titanium-oxide incorporation homogenously in the framework of CN.

In order to investigate whether C-N framework was maintained after titanium-oxide incorporation, XRD, solid state ^{13}C NMR and FT-IR were performed. As can be seen in the XRD patterns (Figure S1), with the increased amount of the molecular titanium-oxide incorporation, there is still no titanium-based compounds peaks. Although the overall intensity of the XRD patterns decrease gradually with the increased content of titanium-oxide incorporation, the two main peaks were always exist as that in pure 2D g-CN (Figure S1). The (002) peak at about 27.8º was the characteristic stacking peak of the conjugated aromatic system with an interlayer distance of 0.321 nm. The peak located at about 13.0º，corresponding to 0.681 nm，is derived from the in-plane lattice planes in g-CN the crystal.[26] The XRD results clearly illustrated that molecular titanium-oxide incorporation in 2D CN would not destroy the basic building structure of the C-N framework. This result was also confirmed by solid state ^{13}C NMR spectra in Figure 1F. The two main peaks in the solid state ^{13}C NMR spectra of 2D CN and TiO-CN2 were similar. The first peak at δ=164.7 ppm is assigned to C atoms in ($CN_2(NH_X)$) and the second peak at δ=164.7 ppm is attributed to the C atoms in (CN_3).[27] Also，the structure of the 2D TiO-CN was further characterized by FT-IR spectra (Figure 1G). All FT-IR spectra

Table 1. Fit results of the first shell around a Ti absorber of the TiO_2 powder and the prepared sample by the IFEFFIT code.

samples	bonds	N	R (Å)	σ2 (×10^{-3}Å2)	E0 (eV)
TiO_2	Ti-O	6.0 ± 0.3	1.96 ± 0.02	5.8 ± 0.6	-0.3
TiO-CN	Ti-O	1	2.07 ± 0.05	1.0 ± 0.1	-8.0
	Ti-N(1)	3	2.14 ± 0.08	5.0± 0.5	-5.0
	Ti-N(2)	3	2.51 ± 0.09	6.0± 0.6	-5.0

Note: 1) S_0^2 = 0.8 from the fit of the TiO_2 powder was used in the fit of the sample; 2) the coordination number of the first shell of the sample was fixed in order to reduce the varied parameters.

of the obtained samples show the feature bands of tri-s-triazine units at about 800 cm^{-1} and aromatic CN heterocycles between 1600 and 1200 cm^{-1}, similar to those of pure 2D CN polymer.[25] In a word, CN nanosheet with molecular titanium-oxide keeps basic C-N framework well.

It is well known that XAFS is one of the most powerful tools to probe the local electronic and geometrical structures around the selected element.[28-30] To further study the local geometrical structure of Ti-O in the subnanopore of CN nanosheets, we performed XAS measurement of TiO-CN at Ti K-edge and chose the anatase TiO_2 as the reference sample. **Figure 2A** shows the Ti K-edge XANES of the Ti-O structure in the CN compared with the spectrum of the standard sample. XANES of anatase TiO_2 presents a well-defined triple of the pre-edge feature before the main crest, same with the spectrum reported by some literatures.[31, 32] This triple pre-edge feature can be assigned to the distorted TiO_6 configuration. That is, Ti is coordinated by six oxygen atoms. By contrast, Ti-O structure in the CN presents intense single pre-edge feature. It is a typical “fingerprint” pre-edge feature of the non-central symmetry.[32] That means the titanium should coordinate only one oxygen atom out of the CN layer. In order to confirm this configuration of TiO-CN, the XANES spectra at Ti K-edge of TiO_2 and the prepared sample were calculated by the Feff8 code in the framework of the full-potential multiple scattering theories.[33] It can be seen that the most features, especially the pre-edge peaks, of the XANES of both the anatase TiO_2 and the TiO-CN sample, using the local structure obtained from the EXAFS fit as discussed below, have been reproduce successfully as shown in **Figure 2B**. Furthermore, **Figure 2C** gives the Fourier transformation (FT) of its EXAFS oscillation of the prepared sample, compared with the standard anatase TiO_2. In contrast to the anatase TiO_2, FT magnitude of the Ti-oxide structure in the CN presents an only broaden and phase-shift peak. Dismissing of FT peaks of the second (Ti-Ti pair) and higher shells in the TiO-CN were clear evidence that only isolated Ti-oxide species were integrated into the g-CN. Phase shift to the larger in the r-space of the first peak means the longer Ti-O or Ti-N bond length. This is consistent with the proposed configuration that TiO pair in the hole of the g-CN network, in which Ti-N bond length is about 2.38 Å. In fact, the first FT peak of the EXAFS only can be simulated successfully by the configuration with double Ti-N pairs, rather than that of only one Ti-N set. The quality of the EXAFS simulation was also shown in the **Figure S11** and the fit structure parameters were given in Table 1. This result from EXAFS quantitative analysis also confirmed that the isolated Ti-oxide species, Ti only coordinating an O atom, indeed locate in the hole of the g-CN sample. Based on above analyses, the XAFS results clearly verified that the molecular titanium-oxide was successfully incorporated into the subnanopore of CN coordinated by the six nitrogen atoms and one oxygen atom as shown in **Figure 2D**, which

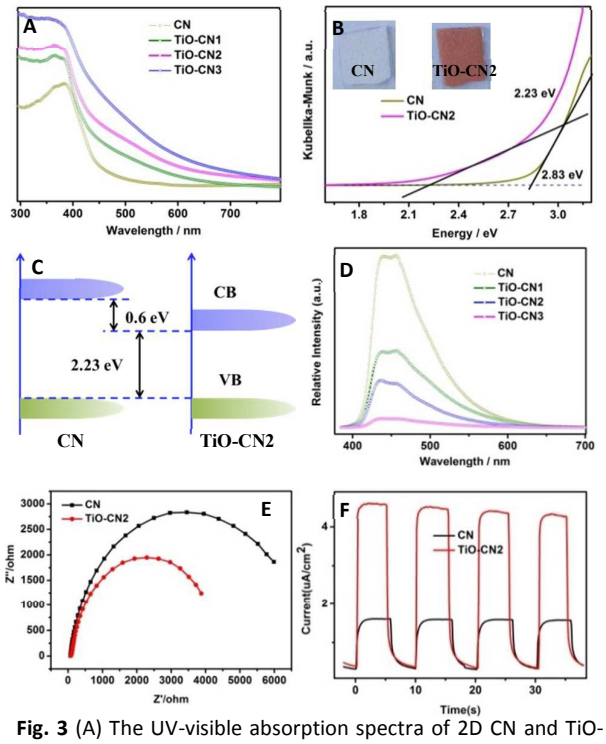

Fig. 3 (A) The UV-visible absorption spectra of 2D CN and TiO-CN. (B) The plot of transformed Kubelka-Munk function vs photon energy for 2D CN and TiO-CN2. (C) Band structure diagram of 2D CN and TiO-CN2. (D) Fluorescence emission spectrums of 2D CN and TiO-CN samples. (E) EIS and (F) photocurrent responses of CN and TiO-CN2 electrode.

was also consistent with the results from XPS (see supplementary information in S4) and HAADF-STEM.

Controllable subnanopore engineering with molecular titanium-oxide incorporation into the "nitrogen pots" of CN nanosheets provided the opportunity to finely tune the electronic band structure of 2D CN. The electronic band structure of CN with different amount of titanium-oxide incorporation was evaluated by UV-visible absorption spectra and room temperature photoluminescence (PL) spectra. As demonstrated in **Figure 3A**, when molecular titanium-oxides were incorporated into the "nitrogen pots" of CN, the molecular titanium-oxide ion would contribute more electrons into CN framework, bringing enhanced π-electron delocalization in the conjugated system with more narrowed bandgap, showing red shift of absorption band edge. Taking 2D CN and TiO-CN2 for example, the bandgap narrow from 2.83 eV to 2.23 eV with the obvious color changing from light yellow to crimson (**Figure 3B**). The VB of both 2D CN and TiO-CN2 were measured by XPS valence spectra (**Figure S12**), revealing the nearly same valence band edge. In that case, based on the bandgap of 2D CN and TiO-CN2, the conduction band edge of TiO-CN2 down-shifts about 0.6 eV with respect to 2D CN as displayed in **Figure 3C**. Additionally, the intensity of PL spectra decreased gradually when increasing the titanium-oxide incorporation content, illustrating effective restrainment of the recombination rates of photogenerated carriers after the subnanopore engineering.[25] To further evaluate the photo-excited charge carries migration, electrochemical impedance spectroscopy (EIS) and photocurrent responses of CN and TiO-CN2 electrodes were performed, revealing

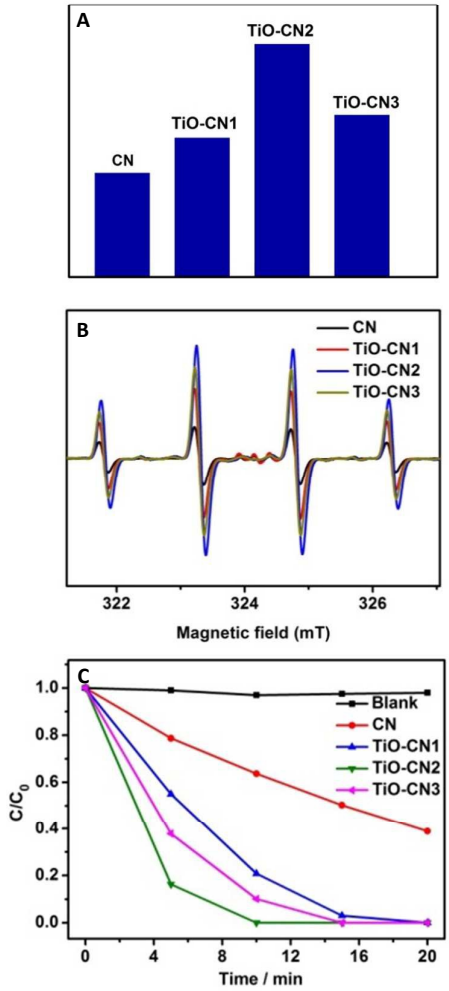

Fig. 4 (A) Comparison of PL relative intensity of 2-hydroxyterephthalic generated by reacting terephthalic acid with •OH radicals in the suspension of CN and TiO-CN nanosheets under visible light (λ > 420 nm) for 25 min. (B) DMPO spin-trapping ESR spectra of samples in aqueous dispersions for DMPO–•OH. (C) Time-dependent photocatalytic degradation of Rhodamine B by the CN and TiO-CN samples under visible light irradiation (λ > 420 nm).

that the mobility of photo-excited charge carriers was promoted after molecular titanium-oxide incorporation (**Figure 3E** and **Figure 3F**). In general, the 2D carbon nitride nanosheets with titanium-oxide incorporation could realize a narrower band gap with optimized separation/recombination rates of photogenerated carriers.

As expected, the electronic structure of 2D CN nanosheets has been effectively tuned by molecular titanium-oxide incorporation and brought about the encouraging results such as improved optical absorption in visible range, enhancement of the separation and migration rate of photo-excited charge carriers, benefiting to photocatalytic reaction. To evaluate the photocatalytic activities of CN and TiO-CN nanosheets, we first monitor an important active species for the decomposing of organic molecules, the amount of •OH radicals by detecting the 2-hydroxyterephthalic acid in

water/terephthalic acid solution.[26] As shown in **Figure 4A**, TiO-CN2 nanosheets show the highest reactivity among all the investigated samples in generating •OH radicals. In order to better understand the capability of generation •OH radical, DMPO spin-trapping ESR measurements were performed for CN and TiO-CN samples.[34,.35] As we known, the DMPO spin-trapping ESR is a more effective technique for detecting the reactive radicals. All ESR spectra as exhibited in Figure 4B show the exclusively 1:2:2:1 quartet signal due to the DMPO-•OH adducts formed upon trapping of the •OH radicals by DMPO molecules. Obviously, as exhibited in **Figure 4B**, ESR spectra show that TiO-CN2 nanosheets exhibited the best capability in generating •OH radical, corresponding well with PL results as shown in **Figure 4A**. Furthermore, the superior photocatalytic performance of the TiO-CN nanosheets was demonstrated by decomposing Rhodamine B under light irradiation. As exhibited in **Figure 4C**, after under visible light irradiation for 5 minutes, the percentage of degraded Rhodamine B by the TiO-CN2 nanosheets could reach as high as 83.7% which is much higher than that of pure CN nanosheets (21.3%). To fully decompose the Rhodamine B under visible light, the TiO-CN2 only need about 10 minutes while the CN samples need more than 45 minutes. Moreover, the TiO-CN2 shows no obvious change after the photocatalytic reactions suggesting its good stability as a photocatalyst. The results of photocatalytic reaction clearly illustrated that the important role of the subnanopore engineering in CN nanosheets which could significantly promoting photocatalytic activity.

In our case, the valance band edge of CN is unchanged (**Figure S12**) and the band gap exhibits a gradual narrowing (**Figure S13**) after molecular titanium-oxide incorporation, suggesting a gradual decreasing of the conduction band edge with increasing molecular titanium-oxide incorporation content in the CN nanosheets. The successful incorporation of molecular titanium-oxide into subnanopore has effectively tuned electronic band structure of 2D carbon nitride nanosheets with band gap narrowing (increasing the visible light absorption). Also, the radiative recombination of photo-excited electrons and holes was greatly decreased as exhibited in **Figure 3D**. Both of them are favorable for the •OH generation (improving the photocatalytic activity). However, the bandgap narrowing would also induce decreasing of conduction band edge of CN nanosheets (**Figure 3C**). For the photocatalysts, a lower of the conduction band gap edge means a weaker reduction ability of the electrons which generated from the conduction band.[36] Obviously, the weaker reduction ability of the electron which generated from the conduction band is unfavorable for the •OH generation (decreasing the photocatalytic activity). Thus, to get better photocatalytic performance, there should be a compromise between the narrowing of the band gap of TiO-CN samples and the reduction ability of their photo-excited electrons. Of note, TiO-CN2 presents the best photocatalytic in our investigated system due to its good balance between a wide light absorption and strong reduction ability.

Conclusions

In conclusion, controllable subnanopores engineering, as a new strategy to regulate the electronic structure of 2D subnanoporous nanomaterials, has been realized in the 2D carbon nitride ultrathin nanosheets by molecular titanium-oxide incorporation. The successful incorporation of titanium-oxide into subnanopore has effectively tuned the electronic band structure of 2D carbon nitride nanosheets with the band gap narrowing and improved its photocatalytic activity under visible light. Introducing of foreign molecular group in subnanopores would pave a new way to regulating electronic structure of 2D nanomaterials catering for energy and catalytic applications.

Acknowledgements

This work was financially supported by the National Basic Research Program of China (2015CB932302), National Natural Science Foundation of China (No. 21222101, U1432133, 11132009, 21331005, 11321503, J1030412), Chinese Academy of Science (XDB01020300) , the Fok Ying-Tong Education Foundation, China (Grant No.141042), and the Fundamental Research Funds for the Central Universities (No. WK2060190027).

References

1 K. S. Novoselov, A. K. Geim, S. V. Morozov, D. Jiang, Y. Zhang, S. V. Dubonos, I. V. Grigorieva, A. A. Firsov, *Science* **2004**, 306, 666-669.
2 Q. H. Wang, K. Kalantar-Zadeh, A. Kis, J. N. Coleman, M. S. Strano, Nat. *Nanotechnol.* **2012**, 7, 699-712.
3 M. Chhowalla, Z. Liu, H. Zhang, *Chem. Soc. Rev.* **2015**, 44, 2584-2586.
4 K. Xu, P. Chen, X. Li, C. Wu, Y. Guo, J. Zhao, X. Wu, Y. Xie, *Angew. Chem.Int. Ed.* **2013**, 52, 10477-10481.
5 Y. Du, Z. Yin, J. Zhu, X. Huang, X.-J. Wu, Z. Zeng, Q. Yan, H. Zhang, *Nat. Commun.* **2012**, 3, 1177.
6 Z. Fan, X. Huang, C. Tan, H. Zhang, *Chem. Sci.* **2015**, 6, 95-111.
7 D. Voiry, H. Yamaguchi, J. Li, R. Silva, D. C. B. Alves, T. Fujita, M. Chen, T. Asefa, V. B. Shenoy, G. Eda, M. Chhowalla, *Nat. Mater.* **2013**, 12, 850-855.
8 Y. Guo, K. Xu, C. Wu, J. Zhao, Y. Xie, *Chem. Soc. Rev.* **2015**, 44, 637-646.
9 M. Chhowalla, H. S. Shin, G. Eda, L.-J. Li, K. P. Loh, H. Zhang, *Nat. Chem.* **2013**, 5, 263-275.
10 C. Lin, X. Zhu, J. Feng, C. Wu, S. Hu, J. Peng, Y. Guo, L. Peng, J. Zhao, J. Huang, J. Yang, Y. Xie, *J. Am. Chem. Soc.* **2013**, 135, 5144-5151.
11 M. Du, X. Li, A. Wang, Y. Wu, X. Hao, M. Zhao, *Angew. Chem.Int. Ed.* **2014**, 53, 3645-3649.
12 D. C. Elias, R. R. Nair, T. M. G. Mohiuddin, S. V. Morozov, P. Blake, M. P. Halsall, A. C. Ferrari, D. W. Boukhvalov, M. I. Katsnelson, A. K. Geim, K. S. Novoselov, *Science* **2009,** 323, 610-613.
13 D. Voiry, A. Goswami, R. Kappera, e. SilvaCecilia de Carvalho Castro, D. Kaplan, T. Fujita, M. Chen, T. Asefa, M. Chhowalla, *Nat. Chem.* **2015**, 7, 45-49.
14 D. Kiriya, M. Tosun, P. Zhao, J. S. Kang, A. Javey, *J. Am. Chem. Soc.* **2014**, 136, 7853-7856.
15 S. W. Han, Y. H. Hwang, S.-H. Kim, W. S. Yun, J. D. Lee, M. G. Park, S. Ryu, J. S. Park, D.-H. Yoo, S.-P. Yoon, S. C. Hong, K. S. Kim, Y. S. Park, *Phys. Rev. Lett.* **2013**, 110, 247201.
16 C. Backes, N. C. Berner, X. Chen, P. Lafargue, P. LaPlace, M. Freeley, G. S. Duesberg, J. N. Coleman, A. R. McDonald, *Angew. Chem.Int. Ed.* **2015**, 54, 2638-2642.
17 I.-Y. Jeon, M. Choi, H.-J. Choi, S.-M. Jung, M.-J. Kim, J.-M. Seo, S.-Y. Bae, S. Yoo, G. Kim, H. Y. Jeong, N. Park, J.-B. Baek, *Nat. Commun.* **2015**, 6, 7123.
18 J. Xie, S. Li, R. Wang, H. Zhang, Y. Xie, *Chem. Sci.* **2014**, 5, 1328-1335.
19 K. Xu, X. Li, P. Chen, D. Zhou, C. Wu, Y. Guo, L. Zhang, J. Zhao, X. Wu, Y. Xie, *Chem. Sci.* **2015**, 6, 283-287.
20 C. Zhang, N. Mahmood, H. Yin, F. Liu, Y. Hou, *Adv. Mater.* **2013**,

25, 4932-4937.
21 G. Das, B. P. Biswal, S. Kandambeth, V. Venkatesh, G. Kaur, M. Addicoat, T. Heine, S. Verma, R. Banerjee, *Chem. Sci.* **2015**, 6, 3931-3939.
22 P. Kissel, D. J. Murray, W. J. Wulftange, V. J. Catalano, B. T. King, *Nat. Chem.* **2014**, 6, 774-778.
23 L. Hao, J. Ning, B. Luo, B. Wang, Y. Zhang, Z. Tang, J. Yang, A. Thomas, L. Zhi, *J. Am. Chem. Soc.* **2015**, 137, 219-225.
24 J. Mahmood, E. K. Lee, M. Jung, D. Shin, I.-Y. Jeon, S.-M. Jung, H.-J. Choi, J.-M. Seo, S.-Y. Bae, S.-D. Sohn, N. Park, J. H. Oh, H.-J. Shin, J.-B. Baek, *Nat. Commun.* **2015**, 6, 6486.
25 X. Zhang, X. Xie, H. Wang, J. Zhang, B. Pan, Y. Xie, *J. Am. Chem. Soc.* **2013**, 135, 18-21.
26 P. Niu, L. Zhang, G. Liu, H.-M. Cheng, *Adv. Funct. Mater.* **2012**, 22, 4763-4770.
27 Y. Cui, Z. Ding, X. Fu, X. Wang, *Angew. Chem.Int. Ed.* **2012**, 51, 11814-11818.
28 T G. Yin, M. Nishikawa, Y. Nosaka, N. Srinivasan, D. Atarashi, E. Sakai, M. Miyauchi, *ACS Nano* 2015, 9, 2111-2119.
29 A. Zitolo, V. Goellner, V. Armel, M.-T. Sougrati, T. Mineva, L. Stievano, E. Fonda, F. Jaouen, *Nat. Mater.* 2015. DOI: 10.1038/NMAT4367.
30 K. Xu, P. Chen, X. Li, Y. Tong, H. Ding, X. Wu, W. Chu, Z. Peng, C. Wu, Y. Xie, *J. Am. Chem. Soc.* **2015**, 137, 4119-4125.
31 L. A. Grunes, *Phy. Rev. B* **1983**, 27, 2111-2131.
32 F. Farges, G. E. Brown, J. J. Rehr, *Phy. Rev. B* **1997**, 56, 1809-1819.
33 A. L. Ankudinov, B. Ravel, J. J. Rehr, S. D. Conradson, *Phy. Rev. B* **1998**, 58, 7565-7576.
34 S. C. Yan, Z. S. Li, Z. G. Zou, *Langmuir* **2010**, 26, 3894-3901.
35 K. Zhao, L. Zhang, J. Wang, Q. Li, W. He, J. J. Yin, *J. Am. Chem. Soc.* **2013**, 135, 15750-15753.
36 T. Inoue, A. Fujishima, S. Konishi, K. Honda, *Nature* **1979**, 277, 637-638.

Graphical Abstract

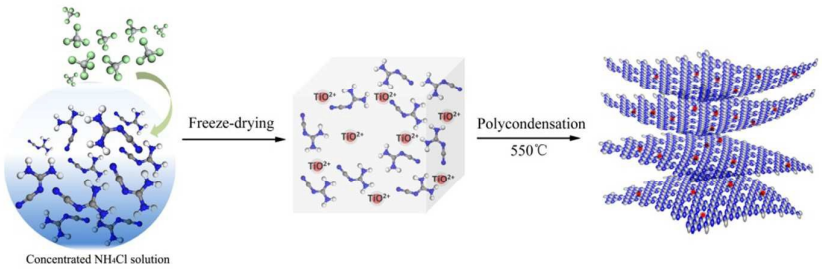

Significantly regulating electronic band structure of 2D carbon nitride nanosheets via controllable subnanopore engineering by incorporation of molecular titanium-oxide which brought about enhanced photocatalytic activity has been realized. Subnanopore engineering would be a new pathway to modulate the intrinsic physical properties of 2D nanomaterials.